Evaluating Kube and Pentland's Fractal Imaging Model

G. McGunnigle M.J. Chantler

G. McGunnigle and M.J. Chantler are with the Department of Computing and Electrical Engineering, Heriot Watt University, Riccarton, Edinburgh EH14 4AS, United Kingdom. E-mail: gmg@cee.hw.ac.uk .

Abstract

The aim of this paper is to assess the validity of a model, proposed by Kube and Pentland [1], that relates a rough surface to its image texture. Simulation was used to assess whether a linear approximation is appropriate, and whether the optimal linear filter agrees with the predictions of Kube and Pentland's model. The predictions of the model about image directionality were also assessed on real images. It was found that a linear model is capable of modelling the imaging process for surfaces of moderate roughness and Lambertian reflectance, and that, subject to a small modification, Kube and Pentland's model accurately predicts the relationship between surface and image spectra.

Keywords

Texture analysis, image models, rough surfaces.

I. Introduction

A large class of visual textures are formed by the interaction of light with natural rough surfaces and several authors have used synthetic textures produced by rendering fractal surfaces [2][3]. However, although Kube and Pentland's paper is expressed in terms of fractals, they develop a frequency domain model (Case 1) that provides an analytical link between surface and image spectra. The analytical nature of this model results in predictions that are both testable and relevent to texture analysis. This paper validates the model by assessing its assumptions using synthetic data and testing whether the model's predictions are observable for real textures.

Where the model is valid, it is an extremely powerful and useful tool for texture analysis. It allows the formation of a coherent spectral model of texture formation that extends from the physical surface to image classification, see [4]. Several authors have shown that image texture can be dramatically affected by the relative orientation of the surface and the illuminant [5],[6],[7], Kube and Pentland's model accurately predicts many of these effects on both the image and features derived from it. In [8] van Ginneken et al. developed a model describing the gray level histogram of a rough surface texture under variations of irradiation and viewing direction. In [9] the effect of variations in the irradition and viewing directions on the correlation length of the image is modelled. It is interesting to compare Pentland and Kube's spectral model with these models. Kube and Pentland model a more constrained system; assuming the viewing direction to be perpendicular to the surface plane and ignoring shadowing. To balance these constraints the Kube and Pentland model has greater predictive ability—it is able to predict the image of a specific surface—rather than a set of statistics. Furthermore, the inverted model can be used to reduce the effect of directional illumination [10] or to estimate the surface height function from its image [11]. In the context of our research, i.e. relatively constrained inspection tasks, the predictive abilities of Pentland and Kube's model outweigh its constraints. Given the potential usefulness of this model, it is worthy of further investigation.

Kube and Pentland's frequency domain model is derived algebraically from a first order, i.e. local, approximation to the rendering function. The validity of the spectral model depends on the accuracy of this linearisation and the emphasis of this paper will be on testing the approximation. We initially test whether the image of a rough, Lambertian surface can be accurately approximated with a linear model. The accuracy of a least squares linear mapping from the surface derivatives vector field to the intensity field is measured. This optimal mapping makes no assumptions save that of linearity. By comparing the effect of illuminant tilt on the estimated parameters with the predictions made by the Kube Pentland model we can assess how close Kube and Pentland's analytical model is to the optimal linear case. Although this correspondence emphasises the local behaviour of the frequency domain model, we will also assess its global effects using physically based surface models and we will consider the implications of the global model for texture analysis.

II. Theory

This section discusses two sets of theoretical models: rough surface models and imaging models. This paper is concerned with the interaction of these models to produce visual textures.

A. Surface Models

The topography of rough surfaces is of interest in several fields including scattering theory and tribology and we can draw upon models proposed within these areas. We will assume that the distribution of heights is Gaussian (many naturally occurring rough surfaces fall into this category [12]) and that the surface is differentiable. A Gaussian signal may be completely characterised by its second order statitics, i.e. its autocorrelation function, or equivalently its power spectrum—assuming the signal is wide-sense stationary.

Several models have been proposed that are stated in terms of the power spectrum. Sayles suggested that the surface profiles of many rough surfaces exhibit an inverse square relationship between frequency and power [13]. The two dimensional form is shown in (1) and a realisation of the model, generated from the specified power spectrum and a random phase spectrum, then rendered using Lambert's law, is shown in Figure 1. Mulvanney developed a related model where the spectrum is white below a cut-off frequency, and obeys a power law above that frequency [14]. The two dimensional form is shown in (2) and a rendered instance with a cut-off frequency of 12 cycles per image (c/i) is shown in Figure 2.

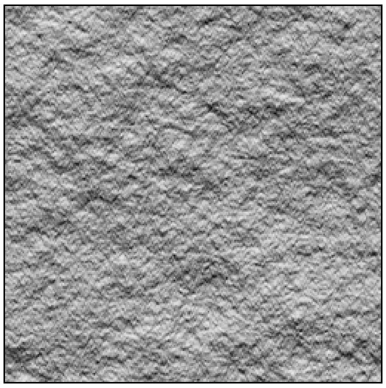

Fig. 1. Rendered Sayles surface

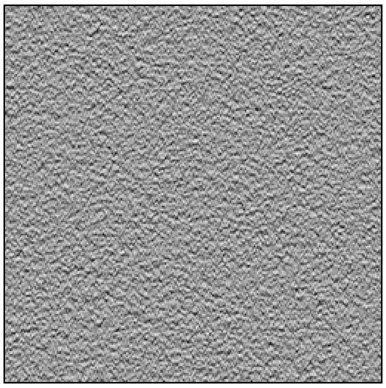

Fig. 2. Rendered Mulvanney type surface

$$S_{2d}(\omega) = \frac{k}{\omega^3} \tag{1}$$

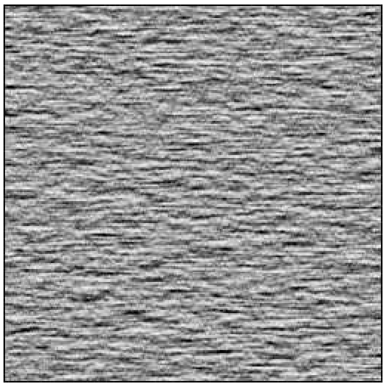

Fig. 3. Rendered Ogilvy type surface

$$S_{2d}(\omega) = k\left(\frac{\omega^2}{\omega_c^2} + 1\right)^{-\frac{3}{2}} \tag{2}$$

where

$S_{2d}(\omega)$	is the two dimensional power spectrum
ω	is the radial frequency
ω_c	is the cut-off frequency
k	is a constant

Although many surfaces are at least approximately isotropic, an important class are directional. Ogilvy suggests a model of directional surfaces where the cut-off frequency is a function of polar angle [12]. The algebraic expression of Ogilvy's model is shown in (3). A surface generated using this model with cut-off frequencies 5 and 12 c/i is shown in Figure 3.

$$S_{2d}(u, v) = \frac{k}{(u_c^2 + u^2)(v_c^2 + v^2)} \tag{3}$$

where

u and v	are the cartesian frequency coordinates
u_c and v_c	are the cut-off frequencies in the x and y directions.
k	is a constant

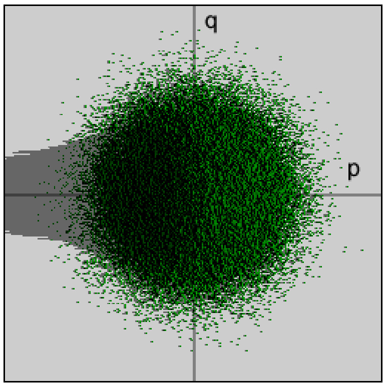

Fig. 4. Scatter plot of slopes from a Sayles surface.

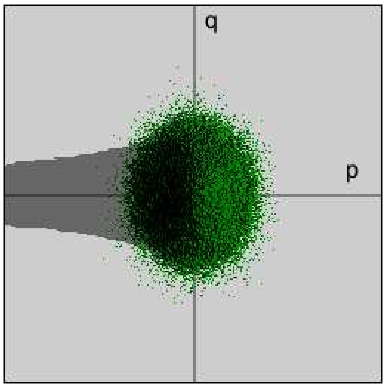

Fig. 5. Scatter plot of slopes from an Ogilvy surface.

Although no single parameter is sufficient to fully describe a textured surface, it may capture important characteristics. Except in the case of (cast) shadowing, the intensity of a point on the image is a function of the surface derivatives of the corresponding surface facet rather than its height. Unlike height, surface slope is a directional parameter, and therefore can indicate the presence of surface directionality. The root mean square (rms) slope is therefore a useful parameter in the context of this work.

We adopt p_{rms} and q_{rms} as the standard deviation of the surface partial derivatives measured along the x and y-axes respectively. Scatter plots of the slopes of the Sayles and Ogilvy surfaces are shown in Figures 4 and 5, since differentiation is a linear process, the distributions of p and q are Gaussian. We will assume the directionality of the surface is aligned with the axes such that p and q are uncorrelated. We also assume the surfaces to be globally flat, and that both components of the mean slope are consequently zero, the resulting joint distribution is zero mean and Gaussian. Note that the directionality of the Ogilvy surface is apparent in the asymmetry of its slope distribution. In contrast, the slope distribution of the isotropic surface has n-fold rotational symmetry. The parameters are linked to the surface power spectrum as shown in (4) and (5).

$$p_{rms}^2 = \int \int u^2 S(u,v) du dv \tag{4}$$

$$q_{rms}^2 = \int \int v^2 S(u,v) du dv \tag{5}$$

B. Reflectance Models

This section is divided into two parts, the first considers the intensity of reflected light on a local basis, i.e. the intensity of a surface facet as a function of the surface derivatives, lighting orientation and, in some cases, viewer orientation. The second part, which is derived from the ideas developed by Kube and Pentland, takes a linear approximation to the local function and uses this to develop a transfer function which links the surface spectrum to the image spectrum. In the experimental section we will verify and refine this analytical model using simulation.

B.1 Local Models

We will consider only surfaces with reflectance functions that are diffuse in character. The classical Lambertian model is generally regarded as being an adequate model of diffuse reflection for most computer graphics applications. The Lambertian assumption is also popular within the field of shape-from-shading. More recently, several authors have developed alternative models [15][16][17][18]. However, since Kube and Pentland's model is derived from the Lambertian case, we will retain Lambert's law in this work.

The reflectance function can be conveniently expressed as a reflectance map (see [19]) . This shows the intensity of a facet as a function of its p and q parameters, and assumes the position of the viewer and light source are held constant. It is defined over the same domain as the scatter plots shown in Figures 4 and 5. The reflectance map for a Lambertian facet illuminated from a tilt angle, $\tau = 0°$ and a slant angle of $\sigma = 50°$ is shown in Figure 6, p and q have the same ranges as in Figures 4 and 5.

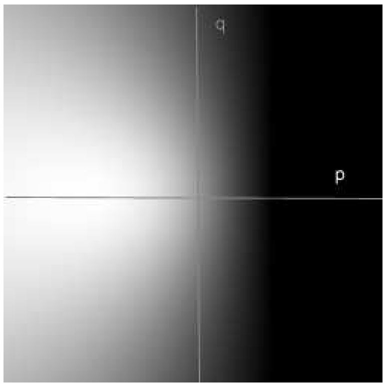

Fig. 6. Reflectance map for Lambertian surface.

B.2 Global Models

B.2.a Kube and Pentland's Model.

Kube and Pentland developed a spectral model (Case 1) that links the surface to the image [1]. The spectral model assumes an orthographic projection onto the x,y plane and that the surface derivatives are small. Kube and Pentland also assume that the illuminant slant angle is greater than 6°. In this correspondence we shall only consider the case where the slant angle is equal to 50°. They also initially assume the surface reflectance to be Lambertian—the image $i(x, y)$ can then be expressed as a function of the illuminant orientation (τ, σ), surface albedo ρ and the surface derivative fields, $p(x, y)$ and $q(x, y)$:

$$i(x,y) = \frac{\rho(-p(x,y)\cos\tau\sin\sigma - q(x,y)\sin\tau\sin\sigma + \cos\sigma)}{\sqrt{p(x,y)^2 + q(x,y)^2 + 1}} \tag{6}$$

A linear approximation (7) to this equation for a given illumination direction (τ, σ) is used to derive a frequency domain expression. The assumption of linearity is valid for surfaces with moderate slopes (< 0.5)[1].

$$i(x,y) = p(x,y)a + q(x,y)b + c \tag{7}$$

where

$a = -\rho\cos\tau\sin\sigma$

$b = -\rho\sin\tau\sin\sigma$

$c = \rho\cos\sigma$

It is worthwhile to note that several authors within the field of shape from shading have also used linearised reflectance maps. Pentland's inversion of the model [11] clearly does so, as does Knill and Kersten's analogous spatial domain approach [21]. Horn also used a linear approximation—though in this case as a simplification for an iterative scheme [20].

Since differentiation is a linear operation (7) can be transformed into the frequency domain to obtain the image power spectrum:

$$I(\omega, \theta) = \rho^2 \omega^2 \cos^2(\theta - \tau) \sin^2 \sigma S(\omega, \theta) \tag{8}$$

where

$S(\omega, \theta)$	is the surface power spectrum
$I(\omega, \theta)$	is the image power spectrum
ω	is radial frequency
θ	is polar angle

The magnitude response of the rendering operation is:

$$M(\omega, \theta) = \omega \rho \cos(\theta - \tau) \sin \sigma \tag{9}$$

B.2.b Optimal Filter Model. More generally, an empirical approach may be pursued where an arbitrary reflectance function is modeled as a linear function of surface derivatives, (10). The filter coefficients, a', b', c' are chosen to minimise the residue quantity shown in (11). This mapping may be defined such that it is optimal in the least squares sense for a given reflectance map and slope distribution. This has some parallels with Knill and Kersten's shape form shading scheme which forms an empirical mapping from the intensity to the surface derivatives—though in that case an adaptive learning algorithm is used [21].

The accuracy of the fit for a given reflectance map is dependent on the location and area of the region that is being approximated. In the case of a texture this is determined by the distribution of surface facets over the pq plane as well as the type of reflectance function. The optimal mapping approximates the entire reflectance map—weighted by the slope distribution function. In contrast, Kube and Pentland make a linear approximation to the reflectance map about its origin.

$$\hat{i}(x,y) = \begin{pmatrix} p(x,y) \\ q(x,y) \\ 1 \end{pmatrix} \begin{pmatrix} a' \\ b' \\ c' \end{pmatrix}^T \tag{10}$$

$$R(x,y) = \Big(\; i(x,y) - \hat{i}(x,y) \; \Big)^2 \tag{11}$$

where *R(x,y)* is the residue image.

The characteristics of a surface will obviously affect the accuracy of the model, however, it is our assertion that they will also affect the *parameters* of that model, i.e. a linear model will be optimal for a particular illumination condition *and for a particular surface.* It follows that the filter coefficients, a', b', c' must be re-estimated for each surface and illumination condition and that it is not meaningful to observe the accuracy of one particular filter for a series of surfaces and illumination conditions.

In this section we have introduced two linear models of the global imaging process. The first, Kube and Pentland's model, (7), is analytical and can be used to predict the image of a surface. The second model, (10), (which we refer to from here as the optimal filter) is empirical, is not predictive but *is* optimal for a given data set. The correspondence between the two models will be used to assess Kube and Pentland's model in the experimental section.

III. EXPERIMENTAL RESULTS

In order to assess Kube and Pentland's linear approach we must consider two questions:
1. Can a linear filter accurately model the Lambertian function for a range of surfaces?
and
2. Do the estimated parameters agree with those predicted by Kube and Pentland's model?

A. Is the linear approximation valid?

Realisations of the Sayles and Ogilvy surfaces with varying degrees of roughness were rendered with the Lambertian model. A least squares approximation to that image was then calculated using (10) and the accuracy of the approximation, i.e. the ratio of the correct signal power to the residue signal power (S/R), measured.

We found that for the isotropic texture, the accuracy of the linear filter falls as the rms slope rises, as shown in Figure 7. However, the filter is able to accurately predict the images of relatively rough surfaces. With anisotropic surfaces the rms slope varies with the measurement direction. We would therefore expect the accuracy of the prediction to vary with the illuminant tilt. The experiment is repeated with the Ogilvy surface rendered under various illumination tilts, Figure 8. As expected there is a tilt dependent variation in the accuracy of the prediction. The filter is most accurate where the illuminant tilt is perpendicular to the grain of the material. If we adopt a nominal minimal accuracy of 10dB we can see that a linear filter is able to model images of surfaces for which the maximum rms slope does not exceed 0.3.

The linear model is a function of the derivatives and its accuracy depends on their first order statistics. The scope of this paper is limited to surfaces whose height, and consequently slope, distributions are Gaussian. In this section we have used surfaces with both isotropic and directional slope distributions of various standard deviations, and have established the types of surface for which an optimal linear filter can accurately predict the image.

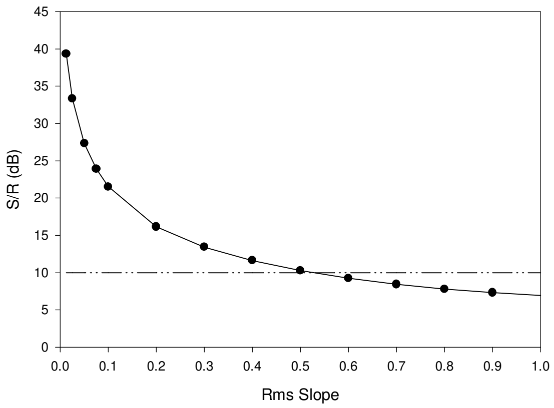

Fig. 7. The accuracy of linear image prediction for an isotropic surface.

B. Is Kube and Pentland's model Optimal?

Having shown that an optimal filter can accurately predict the appearances of a large and useful category of surfaces we now assess how closely the form of the optimal filter resembles that predicted by Kube. Kube and Pentland's model predicts that the a' and

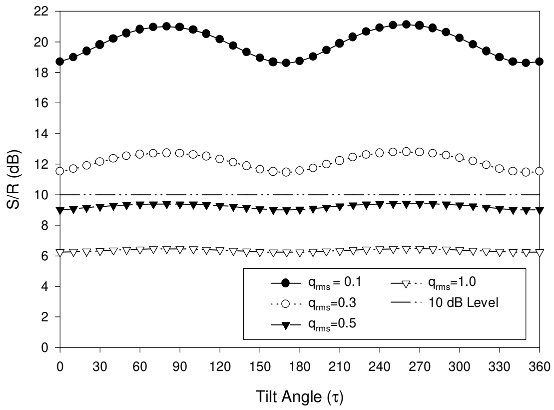

Fig. 8. The variation of prediction accuracy with illuminant tilt and surface slope for the directional texture

b' parameters should vary with $\sin\sigma\cos\tau$ and $\sin\sigma\sin\tau$ respectively. The estimated parameters are plotted against the predictions in Figures 9 and 10 for the isotropic Sayles texture. There does appear to be a good correspondence at all the rms slopes measured, however, the differing slopes of the lines at higher rms slopes is not predicted by Kube and Pentland's model. We can plot the quantity $sqrt(a'^2 + b'^2)$ against the rms slope to show the roughness dependency, Figure 11, (Kube and Pentland's model predicts a constant value of sinσ, independent of rms slope). The roughness dependency is consistent with our earlier assertion that coefficients of the filter, i.e. the parameters of the approximating plane, are dependent both on the reflectance map *and* the slope distribution. Kube and Pentland's model is based on an approximation about the origin, it is optimal for a flat surface, i.e. a surface whose slopes all lie at the origin, as the width of the slope distribution increases, i.e. the surface becomes rougher, Kube and Pentland's model becomes less optimal.

The experiment is now repeated for the directional Ogilvy surface, Figures 12 and 13. Both filter coefficients appear to vary closely with Kube and Pentland's predictions. The values of the *a'* and *b'* parameters at 0° and 90° respectively (their maximum values) are plotted against rms slope, Figure 14. The values are closely related, diverging only slightly for relatively rough surfaces. For this reason we conclude that the modified, roughness

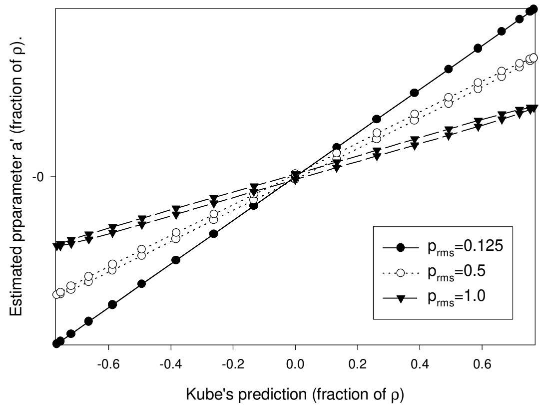

Fig. 9. Estimated filter a' coefficients plotted against Kube and Pentland's $\cos\tau\sin\sigma$ relationship for Sayles surfaces of various roughnesses.

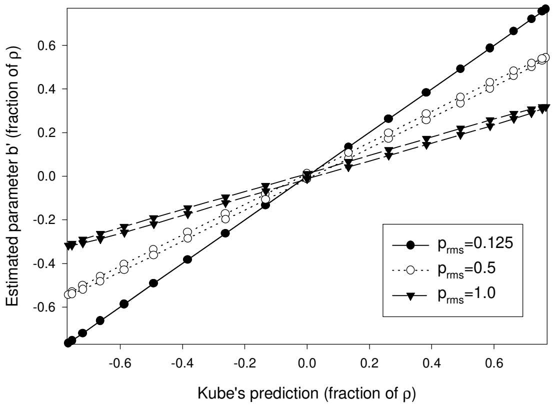

Fig. 10. Estimated filter b' coefficients plotted against Kube and Pentland's $\sin\tau\sin\sigma$ relationship for Sayles surfaces of various roughnesses.

dependent, form of Kube and Pentland's model developed for isotropic surfaces is also valid for directional surfaces. In the case of the random phase Lambertian surfaces used in this work, the qualified Kube expression provides an accurate analytical method for linking surface and image providing that the surface roughness does not exceed 0.3.

C. Consequences of Kube and Pentland's Model for Texure Analyis

In the previous experiments we concluded that, subject to a roughness dependent correction factor, Kube and Pentland's model is able to predict the appearance of a large class of rough surfaces. Modeling the rendering process as a linear filter allows us to relate the spectrum of the surface to that of the image. Kube and Pentland's model predicts

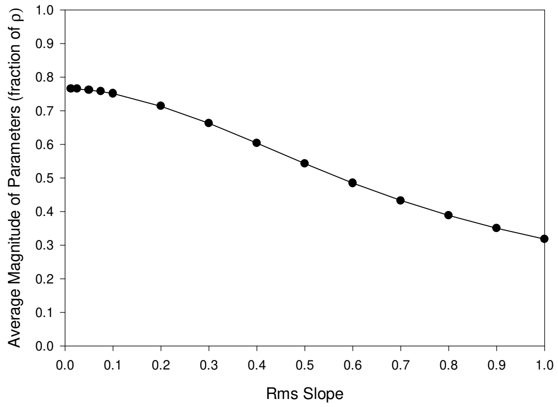

Fig. 11. The dependency of the norm of the filter parameters a' and b' on rms slope for an isotropic surface.(Note that Kube and Pentland's model predicts a constant value of $\rho \sin \sigma = 0.766\rho$ for the norm of a' and b')

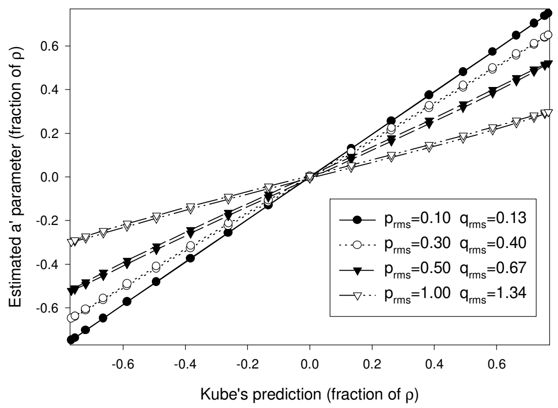

Fig. 12. Estimated filter a' coefficients plotted against Kube and Pentland's -cos(τ) relationship for the directional surface.

that the imaging process acts as a directional high pass filter. In this section we consider the directional and radial properties of the image spectra of the three exemplar textures.

We initially consider the radial spectra of the isotropic surfaces—measured by integrating the two dimensional power spectrum over angle and plotting the result against radial frequency, Figure 15. The Sayles surface with a power roll-off of 3.0 gives rise to an image with roll-off 1.0, this was explicitly predicted in Pentland and Kube's paper. Unlike the image of the Sayles surface which is low pass in nature, the image of the Mulvanney surface is bandpass, with the spectrum increasing with frequency to a gentle peak at the break-point frequency before falling with a roll-off of 1.0. This gives rise to a slight periodicity

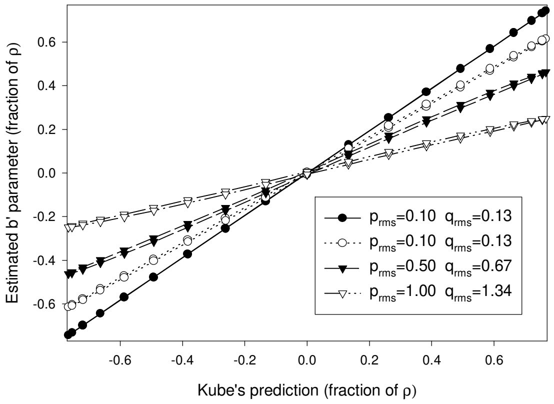

Fig. 13. Estimated filter b' coefficients plotted against Kube and Pentland's -sin(τ) relationship for the directional surface.

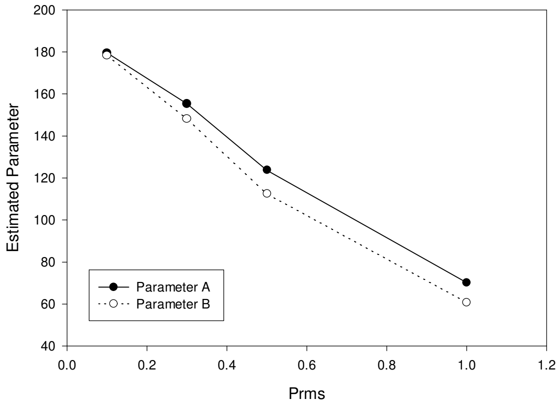

Fig. 14. Variation of a' parameter at 0°and b' parameter at 90°with rms slope for directional texture.

visible in the image.

The directional effects of image formation are shown using a polar plot—formed by integrating the spectra over a radial frequency range and plotting power as a function of angle. The image formed by the isotropic Sayles surface is directional, Figure 16. Since the surface itself is isotropic this directionality is due to the process of image formation. Furthermore, it follows the squared cosine form predicted by Kube and Pentland's model. Consequently if the illuminant tilt angle changes the image directionality is shifted by the corresponding angle.

This is in contrast to the Ogilvy surface, Figure 17. In this case the surface is highly directional and this is the dominant factor in the image directionality with the illuminant

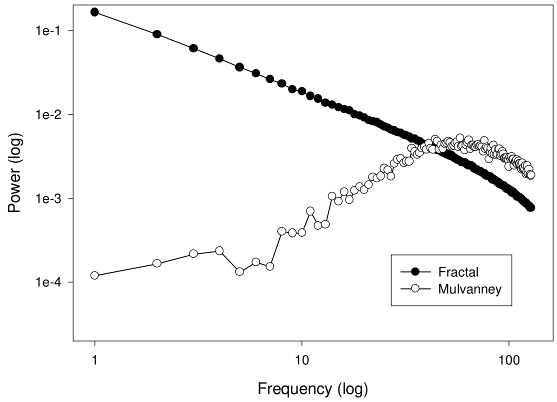

Fig. 15. Radial image spectra of Sayles and Malvanney surfaces.

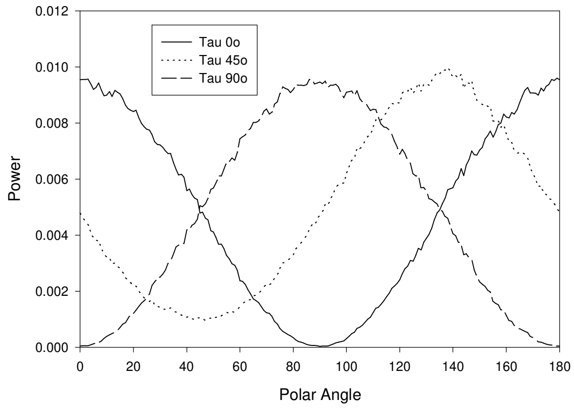

Fig. 16. Polar distribution of image power for Sayles surface illuminated from tilts of 0°,45°and 90°.

having little effect beyond accentuation or attenuation of the directionality inherited from the surface. Thus, when the illuminant vector is perpendicular to surface grain there is a well defined peak, which is attenuated as the illuminant vector becomes parallel to the grain. However, this too is consistent with Kube and Pentland's model.

D. The effect on real textures

Although we are unable to directly measure the surface derivatives of real surfaces, and therefore verify Kube and Pentland's model with real data, we can test some of the predictions of the model. The model predicts that isotropic surfaces will produce images with a cosine distribution of signal energy and that unidirectional surfaces will have images in which the directionality is scaled by the cosine of the angle between the directionality

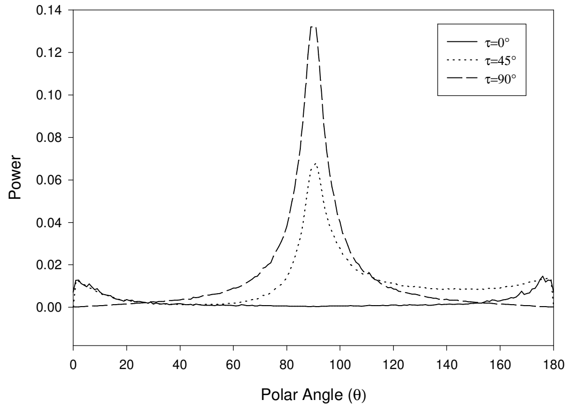

Fig. 17. Polar distribution of power for Ogilvy surface

and the tilt angle of the illumination. We will consider two test surfaces, *Fracture 1*, an approximately isotropic surface and *Ripple 1* a directional surface formed by wave action. Varying the illuminant does not have a dramatic effect on the *Fracture 1* surface beyond a rotation of the image directionality, Figure 18. This rotation can be observed in the polar plots of the *Fracture 1* images, Figure 19. In the case of the *Ripple 1* texture a much more dramatic effect is observed. As the illuminant is revolved towards being collinear with the surface directionality, the directionality in the image becomes attenuated, Figure 20. This effect can also be observed in the textures' polar plots, Figure 21, where the amplitude of the peak is varied but its position remains the same. These results for real textures agree both with our simulations and the predictions of Kube and Pentland's model.

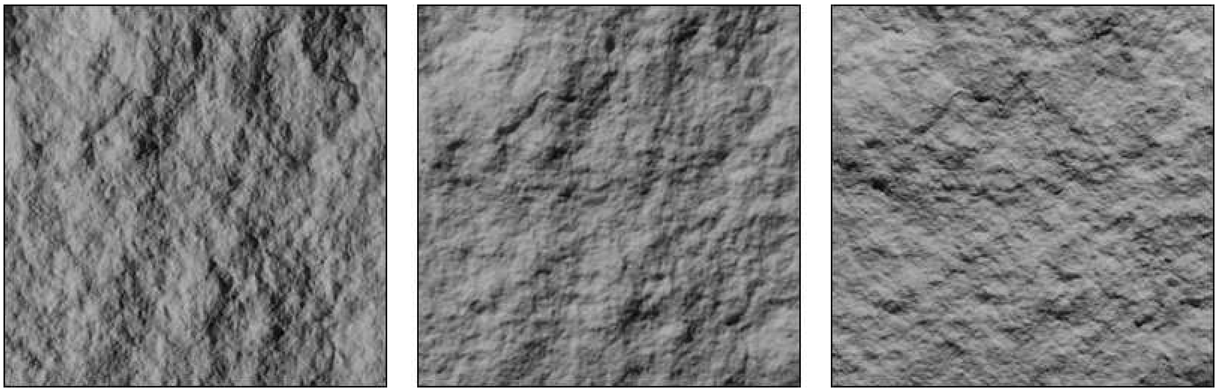

Fig. 18. Fracture 1 sample illuminated from $\tau = 90°$, $135°$ and $180°$

As additional experiments we imaged nine surfaces illuminated at tilt intervals of $15°$ in

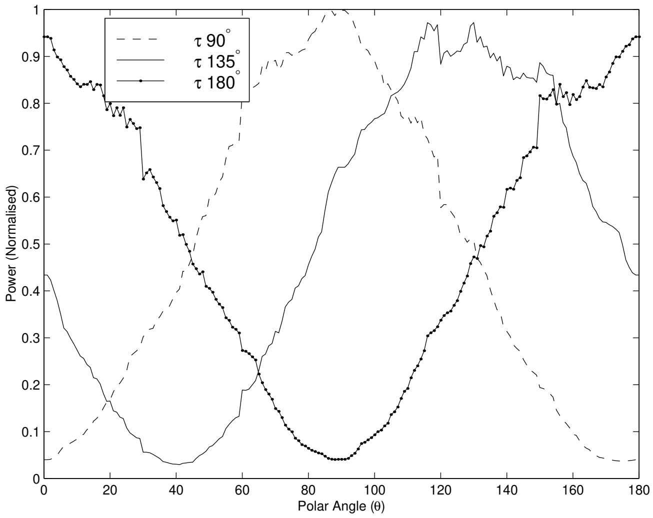

Fig. 19. Polar spectra of Fracture 1 images.

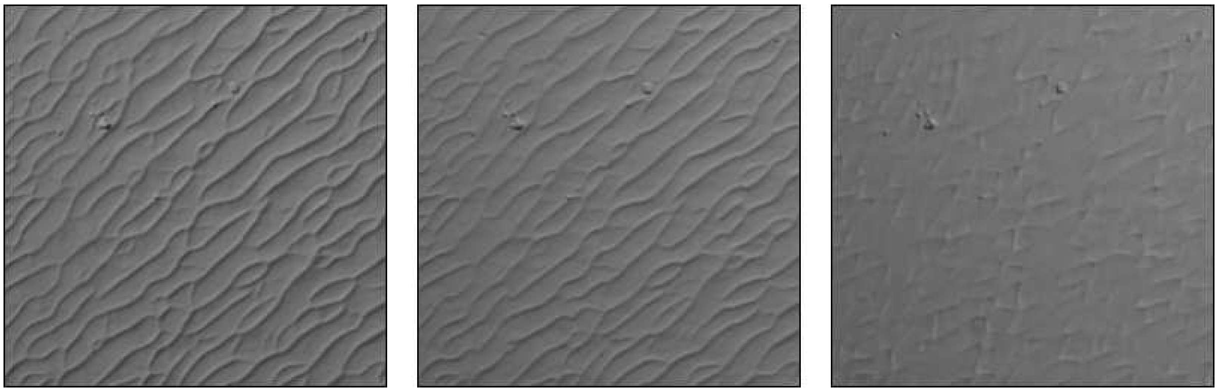

Fig. 20. Ripple 1 sample illuminated from $\tau = 135°$, $180°$ and $225°$

the range $0°$ to $180°$. The nine surfaces are arranged into three classes: *Fractures* Figure 22, *Ripples* Figure 23, and *Grounds* Figure 24. The surfaces are shown illuminated from a tilt angle perpendicular to their directionality. For reasons of space we do not show the power spectra of each image in this correspondence. Instead we plot the standard deviation of image intensity as a function of illuminant tilt. The standard deviation of image intensity is the square root of the integral of the image power spectrum—assuming the mean component to be equal to zero. Each measurement of the standard deviation of an image should correspond to the integral of the polar plot over polar angle. For an isotropic surface we would expect this integral to be constant, i.e. independent of

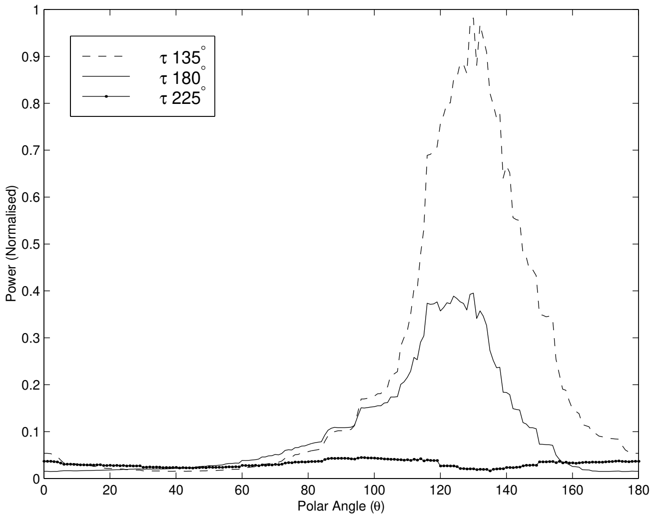

Fig. 21. Polar spectra of Fracture 1 images.

illuminant tilt. For a directional surface the area under the plot varies with tilt. In the extreme case of a unidirectional surface we would expect the standard deviation to vary with the magnitude of the cosine of the angle between the illuminant direction and the surface directionality. The standard deviations of the isotropic *Fracture* images do vary with illuminant tilt, Figure 25, however the degree of variation is small. The directional *Ripple* and *Ground* plots show a much greater degree of variation, Figure 26, Figure 27 which is of the form predicted for a directional surface. The tilt variation of image standard deviation does appear to support the predictions made by Kube and Pentland's model.

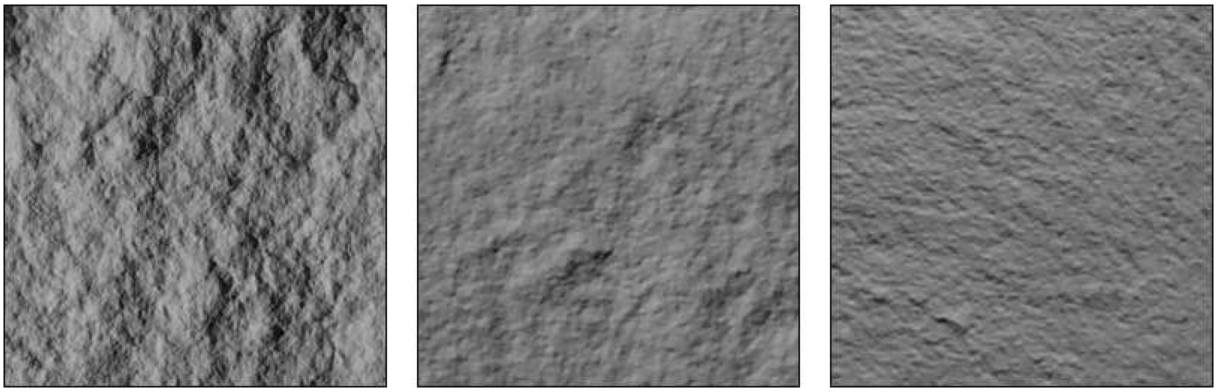

Fig. 22. Fracture surfaces 1-3 illuminated from $\tau = 90°$, $135°$ and $180°$ respectively.

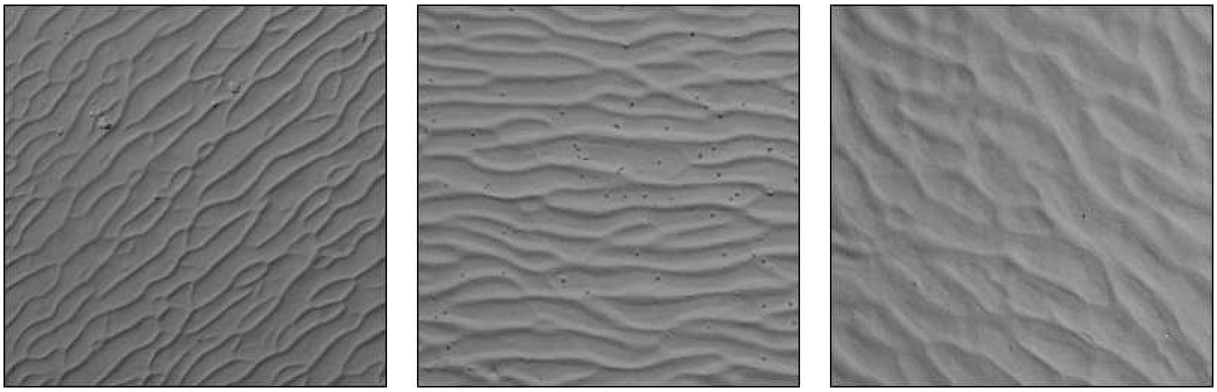

Fig. 23. Ripple surfaces 1-3 illuminated from $\tau = 135°$, $180°$ and $225°$ respectively.

Fig. 24. Ground samples 1-3 illuminated from $\tau = 90°$, $180°$ and $90°$ respectively.

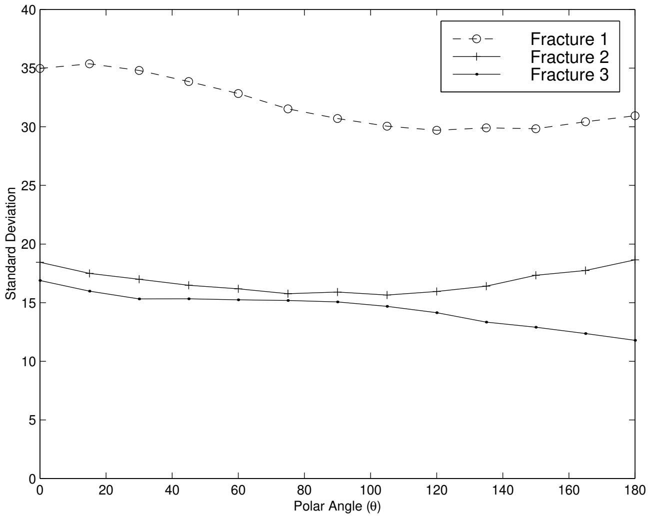

Fig. 25. Standard deviation of Fracture images as a function of tilt.

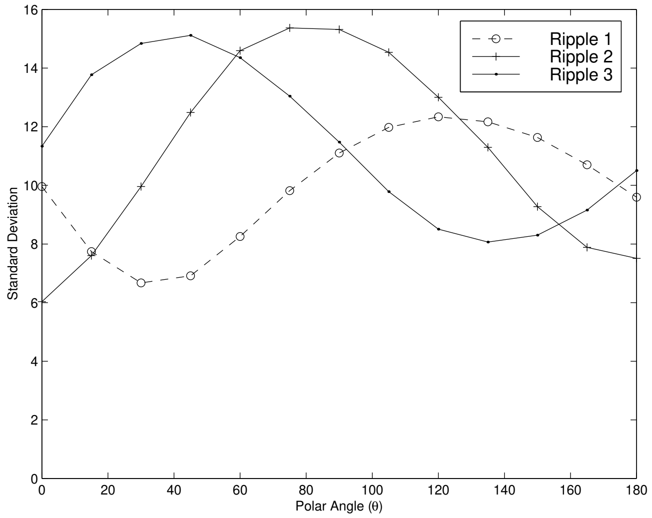

Fig. 26. Standard deviation of Ripple images as a function of tilt.

IV. Conclusions

The experimental work described in this paper strongly supports the use of a linear aproximation to the reflectance function for Lambertian surfaces of moderate roughness, i.e. with rms slopes ≤ 0.3. Furthermore, the predictions made by Kube and Pentland's model about the behaviour of the parameters of that linear approximation are also consistent with our findings, when they are corrected by a roughness dependent scaling factor. Although constructed from a local model, Kube and Pentland's spectral model allows the prediction of global effects. Using physically based surface models we are able to explain the spectral properties of the resulting visual texture. The predictions made by this model, in particular those concerning the interaction of illuminant tilt and surface directionality, are of relevance to the design of texture classifiers which are applied to rough surface textures.

Acknowledgments

This work was partially funded by EPSRC Grant Gr/M73422.

References

[1] P. Kube, A.P. Pentland, *On the Imaging of Fractal Surfaces* , IEEE Trans. Pattern Analysis and Machine

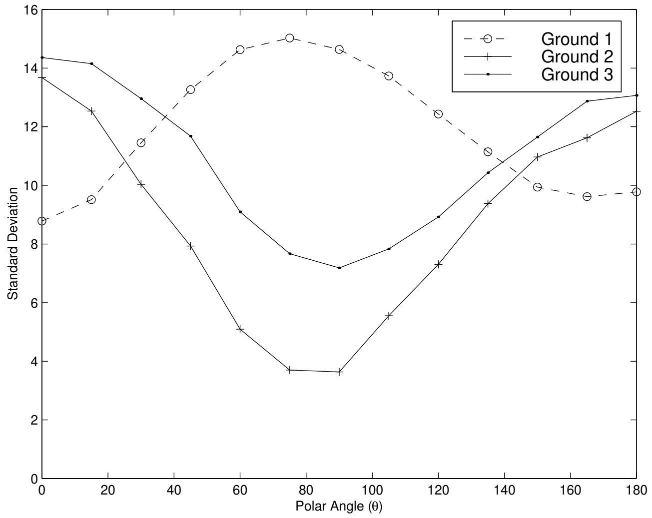

Fig. 27. Polar spectra of Ground images.

Intelligence, 10(5) pp.704-707, 1988.

[2] J.C. Russ, *Fractal Surfaces* , Plenum, 1994, pp.115-138.

[3] L.M. Linnett, *Multi-Texture Image Segmentation*, PhD Thesis, Dept. of Electrical and Electronic Engineering, Heriot Watt University, 1991.

[4] G. McGunnigle, *The Classification of Textured Surfaces Under Varying Illuminant Conditions* , PhD Thesis, Department of Computing Electrical Engineering, Heriot Watt University, April 1998.

[5] M.J. Chantler, *Why illuminant direction is fundamental to Texture analysis*, IEE Proceedings on Vision, Image and Signal Processing, 1995, August Vol.142, No.4, pp.199-206 .

[6] K.J. Dana, B. van Ginneken, S.K. Nayar, J.J. Koenderink *Reflectance and Texture of Real-World Surfaces* , Columbia University Technical Report CUCS-048-96, Dec. 1996.

[7] J.J. Koenderink and A.J. van Doorn *Illuminance texture due to surface mesostructure* , Journal of Optical Society of America A, Vol. 13, No.3, March 1996, pp.452-463.

[8] B. van Ginneken, J.J. Koenderink and K.J. Dana *Texture Histograms as a Function of Irradiation and Viewing Direction* , International Journal of Computer Vision, Vol. 31 (2/3), September 1999, pp.169-184.

[9] K.J. Dana and S.K. Nayar *Correlation Model for 3D Textures* , ICCV '99, pp. 1061-1067, September 1999.

[10] M.J. Chantler, *The effect of variation in illuminant direction on texture classification*, PhD Thesis, Department of Computing Electrical Engineering, Heriot Watt University, August 1994.

[11] A.P. Pentland, *Linear Shape from Shading* , International Journal of Computer Vision, 4, pp.153-162, (1990).

[12] J.A. Ogilvy, *Theory of Wave Scattering from Random Rough Surfaces*, Publisher Adam Hilger, 1991.

[13] R.S. Sayles and T.R. Thomas, *Surface topography as a nonstationary random process*, Nature, Vol.271, 2 February, 1978, pp.431-434.

[14] D.J. Mulvanney, D.E. Newland and K.F. Gill, *A Complete Description of Surface Texture Profiles*, Wear 132 (1989) pp.173-182.

[15] M. Oren and S.K. Nayar *Generalization of the Lambertian Model and Implications for Machine Vision* , International Journal of Computer Vision 14, pp.227-251, 1995.

[16] G. Healey *Using Color for geometry-insensitive segmentation* , Journal of the Optical Society of America A, Vol. 6, No.6, June1989, pp.920-937

[17] L.B. Wolff, *Diffuse-reflective model for smooth dielectric surfaces* , Journal of the Optical Soc. America A, Vol.11, pp.2956-2968, Nov. 1994.

[18] B. van Ginneken, M. Stavridi and J.J. Koenderink *Diffuse and specular reflectance from rough surfaces* , Applied Optics, Vol.37, No.1, pp. 130-139, 1 January 1998.

[19] B.K. Horn, *Robot Vision* , The MIT Press. McGraw-Hill Book Company, 1986.

[20] B.K. Horn, *Height and Gradient from Shading* , International Journal of Computer Vision, 5:1, pp.37-75 (1990).

[21] D.C. Knill and D. Kersten *Learning a Near Optimal Estimator for Surface Shape from Shading* , Computer Vision, Graphics and Image Proceesing, 50, pp.75-100 (1990).